

# Appendix A

## A.1 Synthesis and Characterization

### A.1.1 $(\text{Mg}_{0.16}\text{Fe}_{0.84})\text{O}$

MgO was dried at 1100°C overnight, then stoichiometrically combined with 95% enriched  $^{57}\text{Fe}_2\text{O}_3$  (Advanced Materials Technologies Ltd.) to produce an Fe/(Mg+Fe) ratio of 0.85. After being ground in an agate mortar, the oxide mixture was pressed into a pellet and reduced to form  $(\text{Mg,Fe}^{2+})\text{O}$  in a gas-mixing 1 atm furnace. The pellet was equilibrated at 1400°C for two runs of 20 hours each just above the iron-wüstite fugacity buffer (an oxygen potential of  $10^{-9.6}$  atm). Sample composition and homogeneity were measured using a JEOL JXA-8200 electron microprobe  $(\text{Mg}_{.158(2)}\text{Fe}_{.842(2)})\text{O}$ , where the number in parentheses is the error on the last digit and the oxygen is assumed to be stoichiometric. Ambient pressure unit cell volume was measured with X-ray diffraction (9.79(4) Å/atom), resulting in a density determination of 5.69(7) g/cm<sup>3</sup>. The magnetic signature of iron in our sample was determined by Mössbauer analysis at ambient pressure (Figure 2.6). The absence of a magnetically ordered component indicates that our sample is free of metallic iron and magnetite. Although the black color of the sample indicates that there may be trace amounts of trivalent iron, its concentration is below detection limits of Mössbauer (less than 3%). This will translate to vacancy concentrations of 0-3%, which we include in the density error bar.

In June 2012, a re-measurement of the sample composition revealed the presence of Ti contamination in the sample, previously missed. A revised chemical formula is  $(\text{Mg}_{0.18}\text{Fe}_{0.78}\text{Ti}_{0.04})\text{O}$ , which would correspond to a revised density of 5.7(1) g/cm<sup>3</sup>. With likely errors on each subscript to be

0.01, a more thorough analysis is required to reduce the error bars.

### A.1.2 $(\text{Mg}_{0.06}\text{Fe}_{0.94})\text{O}$

$(\text{Mg}_{0.06}\text{Fe}_{0.94})\text{O}$  was synthesized by the same methods as above, using  $^{57}\text{Fe}$  metal from Isoflex. Microprobe analysis of the synthesized material gives a sample composition of  $(\text{Mg}_{0.0580(9)}\text{Fe}_{0.9420(9)}\text{Si}_{0.0021(9)})\text{O}$ , assuming that the oxygen is stoichiometric. A conventional Mössbauer spectrum (Figure 2.3) taken of the synthesized sample is consistent with divalent iron, and shows no indication of  $\text{Fe}^{3+}$ . A secondary electron image (Figure A.1) taken of the sample before microprobe analysis shows no indication of compositional heterogeneities.

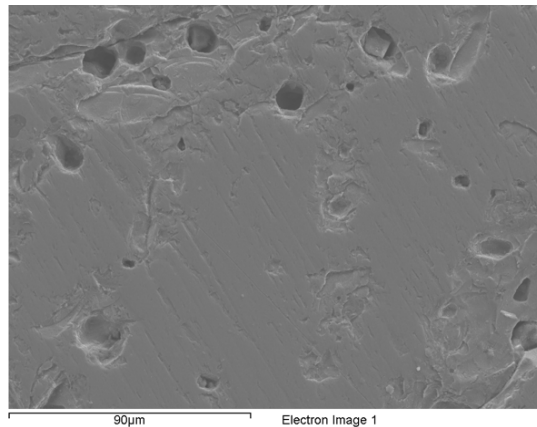


Figure A.1: Secondary electron image of  $(\text{Mg}_{0.06}\text{Fe}_{0.94})\text{O}$ .

### A.1.3 $\text{Fe}_{1-x}\text{O}$

$\text{Fe}_{1-x}\text{O}$  was synthesized in March 2011 using the methods above, at  $1300^\circ\text{C}$ , a lower temperature to account for the melting point of  $\text{FeO}$  of  $1395^\circ\text{C}$ . The synthesis was carried out twice, using both the  $^{57}\text{Fe}_2\text{O}_3$  source and the  $^{57}\text{Fe}$  metal source, as it had been determined that the  $^{57}\text{Fe}_2\text{O}_3$  source was contaminated with Ti. The aim of synthesizing with and without Ti was to determine whether or not the vibrational spectra and subsequent sound velocities were affected by the presence of minor Ti. Room pressure lattice parameter and density are listed in Table A.3.

## A.2 Additional Thermodynamic Parameters

Key thermodynamic information can be directly derived from the partial projected Phonon Density of States using the PHOENIX software (*Sturhahn*, 2000, [www.nrixs.com](http://www.nrixs.com)). More detailed descriptions can be found in *Sturhahn* (2004).

### A.2.1 $(\text{Mg}_{0.16}\text{Fe}_{0.84})\text{O}$

$Pressure^a$ (GPa)	$f_{LM}$	$E_K$ (meV/atom)	$D_{av}$ (N/m)	$f_{LM,Z}$	$E_{K,Z}$ (meV/atom)	$C_{vib}$ ( $k_B$ /atom)	$S_{vib}$ ( $k_B$ /atom)
0	0.7129(8)	14.0(1)	145(5)	0.9069(3)	6.15(9)	2.75(1)	3.57(1)
4.0(3)	0.717(2)	14.0(2)	145(11)	0.9071(7)	6.1(2)	2.8(3)	3.59(3)
11.4(3)	0.713(2)	14.1(3)	169(10)	0.9090(8)	6.3(2)	2.74(4)	2.45(2)
15(3)	0.731(2)	14.2(3)	167(14)	0.9112(8)	6.4(3)	2.73(4)	3.44(3)
21.0(4)	0.727(2)	14.3(3)	183(12)	0.9138(7)	6.7(2)	2.71(3)	3.33(3)
28(2)	0.730(2)	14.2(3)	171(12)	0.9136(8)	6.6(2)	2.72(4)	3.36(3)
41(1)	0.751(2)	14.0(3)	142(14)	0.9153(8)	6.3(2)	2.76(4)	3.36(3)
46(4)	0.778(3)	14.2(3)	177(15)	0.9208(8)	6.9(2)	2.71(4)	3.16(3)
55(3)	0.760(3)	14.2(3)	173(15)	0.9189(9)	6.8(3)	2.72(5)	3.22(3)
65(5)	0.801(3)	14.5(3)	222(12)	0.9263(7)	7.5(2)	2.65(4)	2.95(3)
80(5)	0.814(3)	14.6(3)	229(17)	0.9281(7)	7.7(3)	2.64(4)	2.90(3)
88(4)	0.815(2)	14.9(2)	281(8)	0.9306(5)	8.3(2)	2.59(3)	2.75(2)
97(5)	0.826(2)	15.3(2)	345(13)	0.9336(5)	9.0(2)	2.52(3)	2.61(2)
102(5)	0.834(3)	15.2(4)	326(19)	0.9340(8)	8.8(3)	2.54(4)	2.61(3)
110(4)	0.840(2)	15.4(2)	360(12)	0.9359(4)	9.2(2)	2.50(2)	2.53(2)
121(7)	0.848(2)	15.6(3)	388(16)	0.9377(6)	9.5(2)	2.47(3)	2.45(2)

Table A.1: Thermodynamic parameters calculated directly from the partial-projected phonon density of states of  $(\text{Mg}_{0.16}\text{Fe}_{0.84})\text{O}$ . <sup>a</sup>Pressures were determined from ruby fluorescence before and after the NRIXS measurement, from Table 2.1.  $f_{LM}$  is the Lamb-Mössbauer factor.  $E_K$  is the kinetic energy per resonant atom.  $D_{av}$  is the average force constant of the resonant atom.  $f_{LM,Z}$  is the Lamb-Mössbauer factor at zero Kelvin.  $E_{K,Z}$  is the kinetic energy per resonant atom at zero Kelvin.  $C_{vib}$  is the vibrational specific heat.  $S_{vib}$  is the vibrational entropy per atom.

### A.2.2 (Mg<sub>0.06</sub>Fe<sub>0.94</sub>)O

$Pressure^a$ (GPa)	$f_{LM}$	$E_K$ (meV/atom)	$D_{av}$ (N/m)	$f_{LM,Z}$	$E_{K,Z}$ (meV/atom)	$C_{vib}$ (k <sub>B</sub> /atom)	$S_{vib}$ (k <sub>B</sub> /atom)
0	0.700(1)	14.2(1)	162(5)	0.9076(4)	6.18(8)	2.75(2)	3.57(2)
9.61(2)	0.714(3)	[14.2(3)]	[186(10)]	0.9119(9)	[6.6(2)]	2.72(4)	3.39(4)
42.7(7)	0.773(2)	[14.7(2)]	[261(8)]	0.9237(6)	[7.8(2)]	2.6(3)	2.95(2)
55(1)	0.788(2)	[14.7(2)]	[264(8)]	0.9267(5)	[7.9(1)]	2.61(3)	2.86(2)
64(2)	0.813(2)	[14.8(2)]	[281(8)]	0.9306(5)	[8.3(1)]	2.58(3)	2.73(2)
81.1(8)	0.826(1)	[15.5(2)]	[371(10)]	0.9339(3)	[9.2(1)]	2.50(1)	2.61(1)
81.6(7)	0.828(2)	15.0(2)	300(8)	0.9330(5)	8.6(1)	2.56(2)	2.66(2)

Table A.2: Thermodynamic parameters calculated directly from the partial-projected phonon density of states of (Mg<sub>0.06</sub>Fe<sub>0.94</sub>)O. <sup>a</sup>Pressure determined from in-situ X-ray diffraction, from Table 3.1.  $f_{LM}$  is the Lamb-Mössbauer factor.  $E_K$  is the kinetic energy per resonant atom.  $D_{av}$  is the average force constant of the resonant atom.  $f_{LM,Z}$  is the Lamb-Mössbauer factor at zero Kelvin.  $E_{K,Z}$  is the kinetic energy per resonant atom at zero Kelvin.  $C_{vib}$  is the vibrational specific heat.  $S_{vib}$  is the vibrational entropy per atom.  $E_K$  and  $D_{av}$  reported in brackets denotes values possibly affected by higher energy vibrations not sampled by our limited energy range.

## A.3 Sound Velocities of FeO from Nuclear Resonant Inelastic X-ray Scattering

This section describes the determination of FeO Debye velocities presented in Figure 3.12. NRIXS spectra were taken at Sector 3 of the Advanced Photon Source in August 2011 and March 2012. The volume of FeO at ambient pressure was measured at Sector 12.2.2 of the Advanced Light Source. Using the (111), (200) and (220) reflections, the cubic volume was refined using the *Unit Cell* software. The resulting lattice parameter  $a = 4.306(1)$  corresponds to a composition of  $\text{Fe}_{0.941}\text{O}$  (*McCammon and Liu, 1984*). The volume of FeO at high pressure was measured at Sector 13-ID-D, GSECARS of the Advanced Photon Source in February 2012. Unit cell volumes at high pressure were determined using the rhombohedral reflections: (003), (101), (012), (104), and (110). Density was calculated assuming 0.5(5)% vacancies.

Figure A.2 shows the raw NRIXS spectra of FeO. At ambient pressure, the energy scan range was  $-60 \rightarrow +80$  meV. At higher pressures, the scan range was increased to  $-65 \rightarrow +80$  meV and  $-70 \rightarrow +100$  meV. The partial projected phonon density of states was extracted for each pressure point using the PHOENIX software (*Sturhahn, 2000*) and are presented in Figure A.3.

As described previously, Debye sound velocities were determined using *psvl*. Table A.3 summarizes the density and Debye sound velocities of FeO in addition to the refined unit cell parameters from X-ray diffraction.

$\rho$ (g/cc)	$E_{min} - E_{max}$ meV	$V_D$ (km/s)	Vol/atom $\text{\AA}^3$	$a$ $\text{\AA}$	$c$ $\text{\AA}$
5.99(6) <sup>a</sup>	3.7 – 16.3 <sup>a</sup>	2.87(1) <sup>a</sup>	10.06(2) <sup>a</sup>	4.318(8) <sup>a</sup>	
6.05(2)	3.2 – 17.1	2.88(1)	9.98(4)	4.306(2)	
8.3(1)	4.5 – 14.8	3.73(4)	7.3(1)	2.64(2)	7.26(9)
8.4(1)	4.2 – 19.8	3.88(3)	7.2(1)	2.63(2)	7.21(9)

Table A.3: Summary of FeO density, energy range used to calculate Debye velocities, and Debye velocities. Volume and lattice parameters were refined using the program *Unit Cell* (*Holland and Redfern, 1997*). <sup>a</sup>Density calculated for Ti-containing oxide, estimated to have the chemical formula  $(\text{Fe}_{0.959}\text{Ti}_{0.041(1)})\text{O}$  (*Chen et al., 2012*).

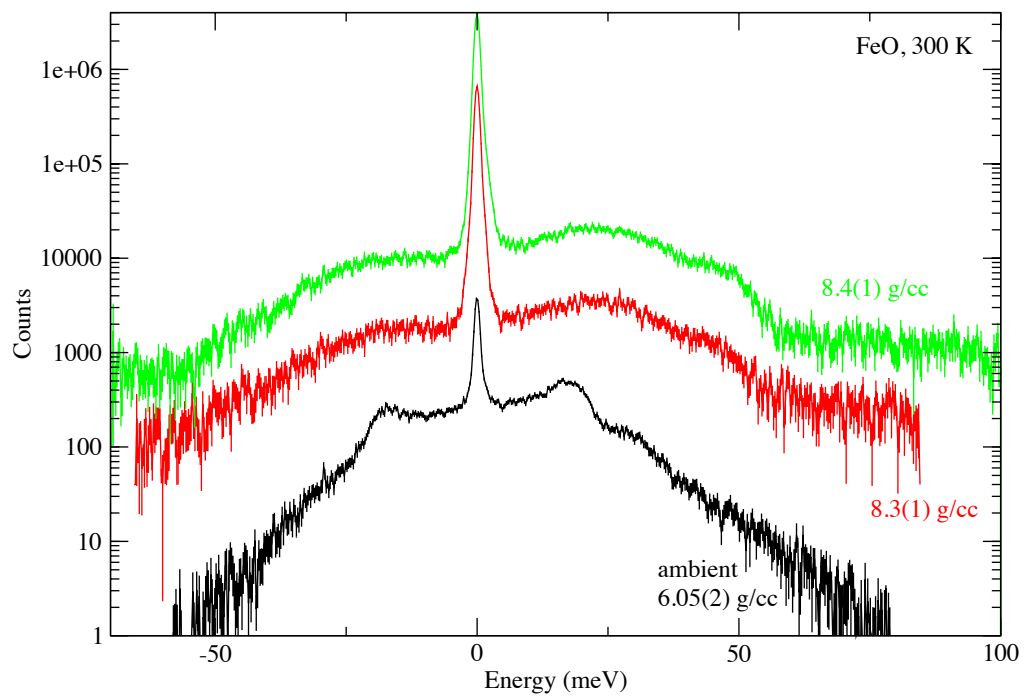


Figure A.2: Raw NRIXS spectra of FeO at 300 K at three pressures.

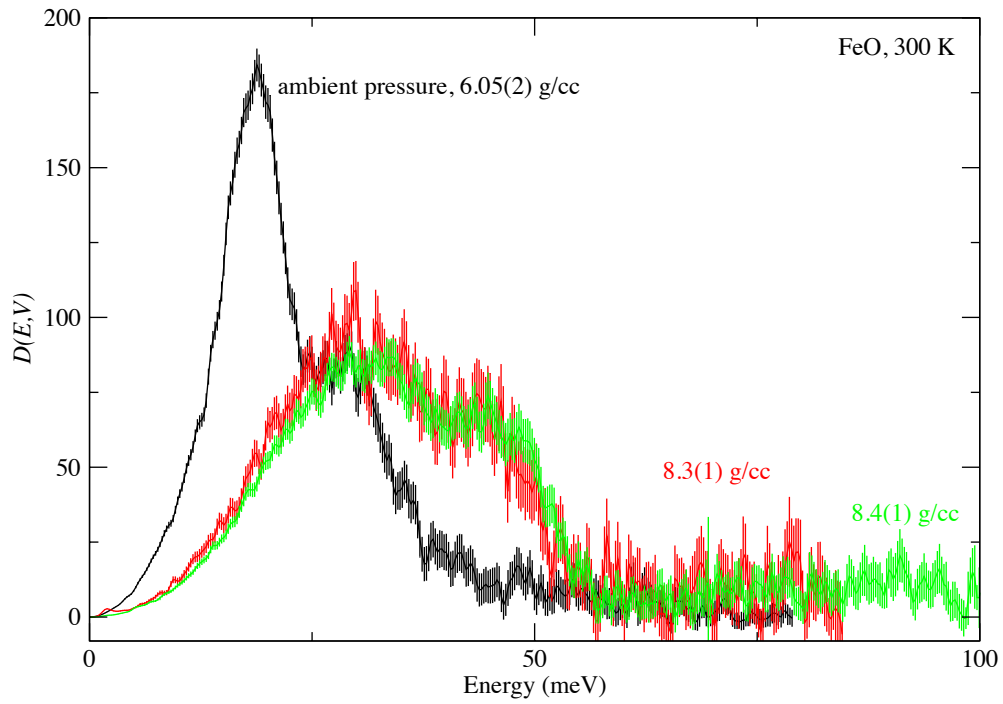


Figure A.3: Partial projected density of states (PDOS) of FeO, extracted from the energy scan using the PHOENIX software (*Sturhahn, 2000*). There is a marked difference in the distribution of vibrations between the ambient pressure spectrum and the high pressure spectra, which is also reflected in the calculated sound velocities. Debye sound velocities determined from the low-energy region of these PDOSs are plotted in Figure 3.12.

